Absence of Large-Scale Displacement of Quinone Q_B in Bacterial Photosynthetic Reaction Centers

Jacques Breton*

Service de Bioénergétique, Bât. 532, CEA-Saclay, 91191 Gif-sur-Yvette Cedex, France

Received January 27, 2004; Revised Manuscript Received February 20, 2004

ABSTRACT: Photosynthesis transforms light into chemical energy by coupling electron transfer to proton uptake at the quinone Q_B. The possibility of initiating this process with a brief pulse of light and the known X-ray structure makes the photosynthetic bacterial reaction center a paradigm for studying coupled electron−proton transfer in biology. It has been established that electron transfer from the primary quinone Q_A to Q_B is gated by a protein conformational change. On the basis of a dramatic difference in the location of Q_B in structures derived from crystals cooled to 90 K either under illumination or in the dark, a functional model for the gating mechanism was proposed whereby neutral Q_B moves 4.5 Å before receiving the electron from Q_A^- [Stowell, M. H. B., McPhillips, T. M., Rees, D. C., Soltis, S. M., Abresch, E., and Feher, G. (1997) *Science 276*, 812−816]. Isotope-edited FTIR difference spectroscopy of Q_B photoreduction at 290 and 85 K is used to investigate whether Q_B moves upon reduction. We show that the specific interactions of the carbonyl groups of Q_B and Q_B^- with the protein at a single binding site remain identical at both temperatures. Therefore, the different locations of Q_B reported in many X-ray crystal structures probably are unrelated to functional electron transfer from Q_A^- to Q_B.

With the rapidly increasing number of three-dimensional structures of large membrane proteins being determined by X-ray diffraction, a major goal in the field of biophysics today is to understand the functions of these proteins at the atomic level. This is a particular challenge when function involves transient interactions with small, mobile molecules. The photosynthetic bacterial reaction center (RC)[1] was the first integral membrane protein to be characterized by X-ray crystallography (*1*−*4*), and is still the subject of detailed studies aiming to relate structure and function. There are now more than 40 entries for bacterial RCs in the Protein Data Bank, and new structures at a resolution approaching 2 Å are currently being generated.

The photosynthetic RC, the primary site of conversion of light energy into chemical energy, contains several chlorophyll and quinone cofactors that catalyze a sequence of light-induced electron and proton transfer reactions (*5*). The structure exhibits a pseudo-C_2 symmetry that relates both the two main L and M subunits and the cofactors, the latter being arranged in two branches, A and B, across the photosynthetic membrane with the 2-fold axis perpendicular to the membrane (Figure 1a). Despite this high degree of structural symmetry, the RC functions in an asymmetric manner with transmembrane electron transfer occurring unidirectionally along the A branch from the primary electron donor (P), a dimer of bacteriochlorophyll molecules, toward the primary quinone Q_A, a ubiquinone-10 (UQ_{10}) molecule in *Rhodobacter sphaeroides*, with a time constant of ∼200 ps. The oxidized primary donor P^+ is reduced by a soluble cytochrome within ∼1 μs, while the electron proceeds to the secondary quinone Q_B (also UQ_{10}) with time constants in the range of 5−200 μs (*6*, *7*). This reaction forms the unprotonated semiquinone Q_B^- which is tightly bound to the RC protein. A second cycle of light-driven electron transfer is coupled to the uptake of two protons from the cytoplasm, forming the ubiquinol (Q_BH_2) (*8*). Finally, the ubiquinol is released into the photosynthetic membrane to activate the cytochrome bc_1 cycle and is replaced with an oxidized quinone from a ubiquinone pool (reviewed in refs *9* and *10*).

One of the most challenging aspects of RC research is unraveling the sequence of reduction and protonation reactions involved in ubiquinol production at the Q_B site, and the accompanying changes in the structure of the protein−cofactor system. Investigation of this process in the RC is made possible by the specific opportunity to trigger the photoreactions quantitatively with brief pulses of light. Elucidation of the mechanism of this reaction at the atomic level would have far-reaching implications because coupled electron and proton transfer reactions are essential processes in many energy-transducing systems. Several observations have indicated that a structural change accompanies the first electron transfer step ($Q_A^-Q_B \rightarrow Q_AQ_B^-$) in the bacterial RC (*7*, *11*−*13*). Notably, the rate of this electron transfer reaction in RCs that have been frozen to cryogenic temperatures under illumination (i.e., in the $P^+Q_B^-$ charge-separated state) is dramatically increased compared to the rate in RCs frozen in the dark (i.e., in the PQ_B state) (*14*). Consistent with the proposal that the rate of the $Q_A^-Q_B \rightarrow Q_AQ_B^-$ reaction at ambient temperature is limited by a conformational change,

* To whom correspondence should be addressed. Telephone: (331) 6908 2239. Fax: (331) 6908 8717. E-mail: cadara3@dsvidf.cea.fr.

[1] Abbreviations: RC, reaction center; P, primary electron donor; Q_A and Q_B, primary and secondary quinone acceptors, respectively; UQ_n, ubiquinone-*n*, 2,3-dimethoxy-5-methyl-6-polyprenyl-1,4-benzoquinone; FTIR, Fourier transform infrared.

10.1021/bi049811w CCC: $27.50
Published on Web 03/06/2004

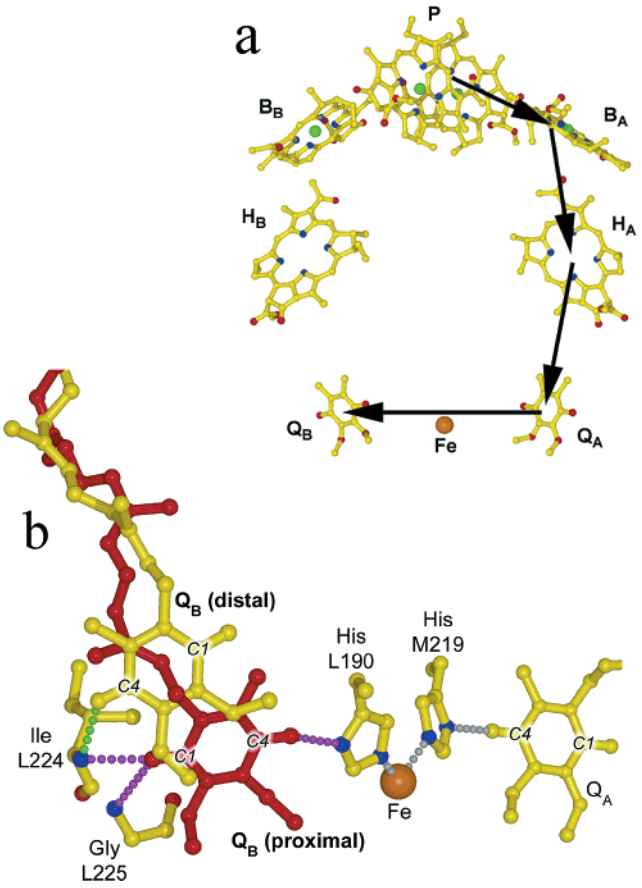

FIGURE 1: (a) Overall organization of the cofactors in the RC of *Rb. sphaeroides*. The bacteriochlorophyll (dimeric primary electron donor P and monomeric B), bacteriopheophytin (H), and ubiquinone (Q) cofactors are arranged around the axis of 2-fold symmetry in two branches (A and B) that span the membrane. The route of electron transfer from P to Q_B along the A branch is shown by the arrows. (b) Distal and proximal binding positions of the Q_B ubiquinone in the RC. When in the distal position (yellow), the C_4═O carbonyl accepts a hydrogen bond (green spheres) from the backbone amide NH group of Ile-L224, while the C_1═O carbonyl is free. When in the proximal position (red), the C_1═O carbonyl is hydrogen-bonded (magenta spheres) to the backbone NH group of Ile-L224 and Gly-L225, while the C_4═O carbonyl is hydrogen-bonded to the side chain of His-L190. The headgroup of the proximal Q_B ubiquinone is arranged approximately symmetrically to that of the Q_A ubiquinone. This figure is courtesy of P. Fyfe (University of Bristol, Bristol, U.K.).

it has been demonstrated that the observed rate of this reaction is independent of the driving force for electron transfer (*15*).

In an attempt to resolve the structural changes that accompany charge separation in the RC, the structure of *Rb. sphaeroides* RCs in single crystals cooled to 90 K under illumination was compared to that in single crystals cooled to 90 K in the dark (*16*). A dramatic difference in the location of Q_B was observed in the two structures (Figure 1b), leading to a functional model in which the secondary quinone was proposed to occupy two distinct positions depending on its reduction state. In this model, the neutral Q_B, located in a "distal" site, must undergo a 180° "propeller twist" and a 4.5 Å displacement toward a "proximal" site for the $Q_A^-Q_B \rightarrow Q_AQ_B^-$ electron transfer step to occur (*16*). As illustrated in Figure 1b, of the two quinone carbonyls (C_1═O and C_4═O), only the latter forms a hydrogen bond with the protein in the neutral Q_B state (distal position), while both carbonyl groups are hydrogen-bonded to the protein in the semiquinone state (proximal position). The motion of Q_B from the distal to the proximal site, possibly in response to Q_A^- formation, was proposed to represent the conformational gate that allows electron transfer to proceed from Q_A^- to Q_B (*15*). This gating mechanism would account for the observation that RCs trapped at low temperatures in the dark, where Q_B is in the distal position are inactive for the $Q_A^-Q_B \rightarrow Q_AQ_B^-$ reaction, but RCs cooled under illumination are frozen in an active state (*14*). On the basis of detailed X-ray studies of Q_B-depleted, Q_B-reconstituted, and Q_B-inhibited RCs from *Rhodopseudomonas viridis*, a mechanistic model involving a similar displacement of Q_B from the distal to the proximal site has also been proposed to accompany the $Q_A^-Q_B \rightarrow Q_AQ_B^-$ electron transfer step in the RCs of this species (*17*, *18*). The conformational gating model has triggered a number of electrostatic and molecular dynamics computational studies aimed at explaining the causes of the change in the position of Q_B, the details of the complex motion (flip and translation) of Q_B, and how this motion relates to the actual opening of the gate (*19*−*25*).

Complementing X-ray crystallography, the binding of quinones (both Q_A and Q_B) in RCs has been investigated in detail by Fourier transform infrared (FTIR) difference spectroscopy (reviewed in ref *26*). IR spectroscopy is an exquisitely sensitive technique for the investigation of atomic interactions and can detect even minute structural changes in the vicinity of functional groups. In the case of a large molecular system such as the RC, the complexity of IR spectra can be overcome by using a difference technique whereby the FTIR spectrum of the ground state of the protein is subtracted from that of an active state, such as a well-defined photoinduced charge-separated state. Using such a procedure, only the groups that alter their molecular vibrations with the change in state contribute to the difference spectrum, while all the absorbance bands from groups that do not participate in the reaction are canceled out. With a combination of this technique and isotope labeling, it is possible to detect and assign vibrational modes of single chemical groups in a protein complex as large as a RC (*26*).

In previous work, RCs reconstituted with ubiquinone-3 (UQ_3) specifically labeled with ^{13}C at either the C_1═O or C_4═O carbonyl (Figure 1b) were used to probe the bonding interactions of the C═O groups of Q_B and Q_B^- in the RCs of two of the most thoroughly investigated species of purple bacteria, namely *Rp. viridis* and *Rb. sphaeroides* (*27*). The observation that in the RCs of both species, both Q_B carbonyl groups exhibit the same frequency of 1641 cm^{-1}, downshifted by 10−20 cm^{-1} compared to the frequency of the free carbonyl groups of the quinone in solution, led to the conclusion that both carbonyl groups of Q_B engage in symmetrical and moderate-strength hydrogen bonds with the surrounding protein (*27*, *28*). Compared to the variable positions of Q_B that had been seen in X-ray structures (*29*), it was proposed (*26*, *27*) that neutral Q_B in both species was likely to be located in the site that is now defined as the proximal site, at a position consistent with the hydrogen bonding pattern involving both carbonyls of the quinone first described (*29*) and discussed (*17*) for *Rp. viridis*. This proposal is supported by recent studies on mutant *Rb. sphaeroides* RCs that compare the location of Q_B derived from crystallographic investigations and from isotope-edited

Q_B^-/Q_B FTIR spectroscopy. In some X-ray crystallographic studies at ambient temperature on dark-adapted crystals of *Rb. sphaeroides* RCs bearing mutations in the vicinity of the quinone sites, Q_B has been found at or close to the proximal position (*30*−*32*). The isotope-edited FTIR fingerprints for the interaction of neutral Q_B with the protein have been measured for two of these mutant RCs (*33*, *34*), and the bonding pattern for both the C_1═O and C_4═O carbonyls of neutral Q_B has been found to be the same as that previously measured for wild-type RCs (*27*).

Although Stowell *et al*. (*16*) noted the strong discrepancy between the positions of the neutral Q_B as derived from FTIR difference spectroscopy at room temperature (*27*) and from X-ray crystallography of cryotrapped intermediates, an explanation for this difference has not been forthcoming. In the work presented here, this issue has been reinvestigated by employing experimental conditions for FTIR spectroscopy that address directly the possibility that Q_B could move upon photoreduction as proposed from the X-ray results (*16*−*18*). Using isotope-edited FTIR difference spectroscopy with site-specifically labeled ubiquinone, the hydrogen bonding states of Q_B and Q_B^- are compared at room temperature, where Q_B is free to move upon photoreduction, and at 85 K, where such a motion cannot occur.

EXPERIMENTAL PROCEDURES

Sample Preparation. RCs were purified and depleted of the quinone Q_B according to the method described in ref *35*. The Q_B site was reconstituted with UQ_3 by adding an ∼10-fold excess of UQ_3 as described previously (*36*). The synthesis and characterization of the ^{13}C-labeled UQ_3 have been reported (*37*). For the IR measurements, 10 μL of a 200 μM RC solution in Tris-HCl (20 mM, pH 7.0) containing 0.02% LDAO was partially dried under argon on a 25 mm diameter CaF_2 disk. The sample was then covered with another CaF_2 disk to form a thin cell, the outer edges of which were sealed with high-vacuum silicon grease.

FTIR Measurements. The measurements were performed with a Nicolet Magna 860 spectrometer equipped with an MCT-A detector. Illumination of the sample was achieved under saturating actinic light using an RG715 cutoff filter and a water filter to prevent heating of the sample. In-house software was implemented to control the electronic shutter and the data acquisition periods of the FTIR spectrometer. A gas convection cryostat operated with liquid nitrogen was used to control the temperature of the sample within ±0.1 °C. Typically, three IR samples of RCs, each reconstituted with one of the three quinone isotopomers, were prepared under closely identical conditions. The samples were mounted on special holders fitting into the cryostat and were kept frozen at −60 °C until they were used. The cryostat temperature was set to 85 K. One of the RC samples was thawed, illuminated at ambient temperature (20 °C) for 15 s, and rapidly (∼1 s) transferred to the cryostat under illumination. The rate of cooling of the sample was adjusted so that a temperature of 100 K was reached after ∼30 min. Liquid nitrogen was then allowed to cover the whole IR sample for a few minutes, at which point the illumination was switched off and the temperature control was set to 85 K. Two hours after the procedure was initiated, the sample temperature was sufficiently stable to start the FTIR measurements. The transmission of the sample at 85 K was measured during periods of 60 s first in the dark, then under illumination, and then in the dark after illumination was switched off to control the relaxation of the sample. Following Fourier transformation, the three single-beam spectra were processed to yield a light-minus-dark and a relaxation-minus-dark ΔA spectrum. A delay of 30 s was introduced before starting the next cycle. For each sample, these cycles were iterated over a period of ∼22 h. At this stage, the sample was removed and stored at −60 °C while the next sample was processed. Each set of three samples was analyzed four times at 85 K and once at 290 K. For the measurements at 290 K, the measuring times within each cycle were set to 30 s and no delay was introduced during the cycles. Eight sets of IR samples from two different batches of RCs were analyzed, and the data were averaged. The resolution is 4 cm^{-1}, and the frequencies are given ±1 cm^{-1}.

RESULTS

Q_B Photoreduction at Room Temperature. In the presence of an excess of ubiquinone to maximize the occupancy of the Q_B site, illumination of purified *Rb. sphaeroides* RCs at ambient temperature with either a single flash or continuous light leads to the formation of the $P^+Q_B^-$ state. This state, which can be generated quantitatively by excitation with saturating light, decays back to the PQ_B ground state with a time constant of 1−5 s (*9*, *10*). The FTIR absorption spectrum of such a RC sample under illumination contains the contribution of vibrational modes of the $P^+Q_B^-$ state, while the FTIR spectrum of the same sample measured in the dark just prior to the illumination contains those of the PQ_B state. The calculated $P^+Q_B^-$-minus-PQ_B difference spectrum (abbreviated as $P^+Q_B^-/PQ_B$ in the following) therefore represents the IR signature of the molecular changes associated only with this specific light-induced transition. In such difference spectra, the bands of the neutral PQ_B state appear as negative contributions and those of P^+ and Q_B^- as positive bands. While the dominating contributions from P^+/P are distributed over the whole spectral range that was investigated, the main C═O and C═C bands associated with Q_B are localized in the 1660−1600 cm^{-1} region, and the coupled C⋯O/C⋯C modes of the semiquinone Q_B^- absorb between 1500 and 1400 cm^{-1} (*26*−*28*, *36*).

$P^+Q_B^-/PQ_B$ FTIR difference spectra measured with saturating continuous illumination at 290 K were recorded for Q_B-depleted *Rb. sphaeroides* RCs reconstituted with UQ_3 that was either unlabeled (Figure 2Aa) or labeled with a single ^{13}C atom at the C_1 (Figure 2Ab) or C_4 (Figure 2Ac) position. Most of the features in the spectra in Figure 2Aa−c are practically identical, as seen by the almost complete overlap of the three spectra. However, small but highly reproducible differences can be detected, notably, the different ratio of the amplitude of the negative bands at 1638 and 1618 cm^{-1}, in the region of absorption of the C═O and C═C vibrations of the neutral quinone (*26*−*28*, *36*). In addition, the amplitude of the positive band at 1478 cm^{-1}, which is close to the position where the main mixed C⋯O/C⋯C mode of the semiquinone Q_B^- absorbs (*26*−*28*, *36*), is larger in the spectrum obtained with the unlabeled quinone (Figure 2Aa) than in the two other spectra (Figure 2Ab,c), while smaller differences are seen between 1450 and 1400 cm^{-1}.

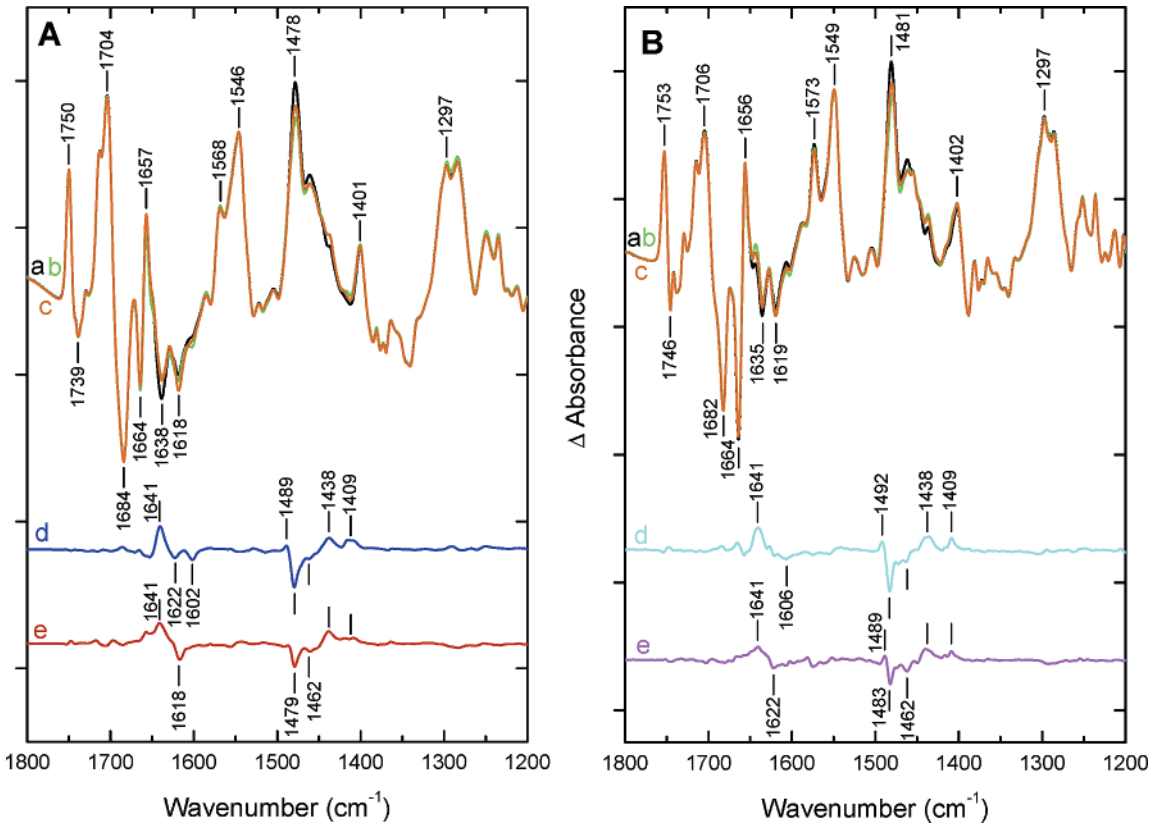

FIGURE 2: FTIR difference spectra corresponding to the light-induced $PQ_B \rightarrow P^+Q_B^-$ charge separation in *Rb. sphaeroides* RCs at 290 K (A) and at 85 K for RCs cooled under illumination (B). The RCs were reconstituted with UQ_3 either unlabeled (a, black) or isotopically labeled with ^{13}C at C_1 (b, green) or C_4 (c, orange). Isotope-edited IR fingerprint spectra for the interactions of Q_B and Q_B^- with the protein at the binding site are calculated as the double-difference spectra (isotopically labeled-minus-unlabeled) for RCs reconstituted with $^{13}C_1$-labeled (Ad, blue; Bd, cyan) and $^{13}C_4$-labeled (Ae, red; Be, magenta) UQ_3, respectively. The amplitude between tick marks represents 1.4×10^{-3} and 10^{-3} absorbance unit in panels A and B, respectively.

These small differences represent the isotope-sensitive vibrational modes of Q_B and Q_B^- that involve displacement of the C_1 and C_4 atoms. They are best visualized by calculating double-difference spectra between a pair of $P^+Q_B^-/PQ_B$ spectra recorded with RCs reconstituted with isotopically labeled or unlabeled quinones. This produces spectra in which all the vibrations that are affected by the $PQ_B \rightarrow P^+Q_B^-$ reaction are canceled out except those modes that involve motion of the C_1 and C_4 atoms of Q_B and Q_B^-. In these double-difference (isotopically labeled-minus-unlabeled) spectra, the IR bands of the neutral unlabeled Q_B now appear with a positive sign, while the downshifted bands of the neutral labeled quinone appear with a negative sign. A reverse situation is found for the bands of the semiquinone. The calculated double-difference spectra for $^{13}C_1$ and $^{13}C_4$ labeling of Q_B are spectra d and e of Figure 2A, respectively. All of the bands that are highlighted in the double-difference spectra (Figure 2Ad,e) are reproducibly observed in several repeats of the same experiment. These bands can be confidently assigned to Q_B and Q_B^- modes not only on the basis of their sensitivity to selective isotope labeling of the added quinone but also because they have been previously observed at the same frequency and with closely comparable absolute and relative intensities in equivalent double-difference spectra calculated from another fully functional state of Q_B, i.e., in Q_B^-/Q_B FTIR spectra of isolated *Rb. sphaeroides* RCs reconstituted with quinones bearing the same ^{13}C label, and generated with a single-turnover saturating flash in the presence of a redox buffer and an external mediator to rapidly reduce P^+ (*27*, *28*; see also Figure 3a,a′). The small spurious bands that are not highlighted in spectra d and e of Figure 2A are assigned for the most part to incomplete cancellation of large signals from either P or P^+ (between 1760 and 1680 cm^{-1}) and from contributions of protein amide I and II modes (around 1660−1650 and 1550 cm^{-1}), respectively, in the $P^+Q_B^-/PQ_B$ FTIR difference spectra.

The isotope-edited double-difference spectra represent highly specific fingerprints for the interactions of Q_B and Q_B^- with the protein at the binding site. In particular, the common positive peak at 1641 cm^{-1} (Figure 2Ad,e) shows symmetrical and moderate-strength hydrogen bonding of both Q_B carbonyls to the protein. On the other hand, the differences in the 1620−1600 cm^{-1} frequency range indicate that the constraints exerted by the protein on the quinone at the level of the C_1 and C_4 atoms are inequivalent (*26*, *27*). For UQ_3 in vitro, the corresponding isotope-edited difference spectra are essentially identical in this spectral range for $^{13}C_1$ and $^{13}C_4$ labeling (*27*), as expected from the equivalent environment of the two carbonyl groups. In contrast to the symmetry seen for Q_B, the corresponding isotope-edited double-difference spectra for the photoreduction of Q_A are characterized by a very large frequency downshift (~60 cm^{-1}) of the C_4═O carbonyl group, while the C_1═O group of Q_A observed at 1660 cm^{-1} is essentially unperturbed compared to that in solution (*33*, *38*). This demonstrates that the Q_A ubiquinone engages in highly asymmetric hydrogen

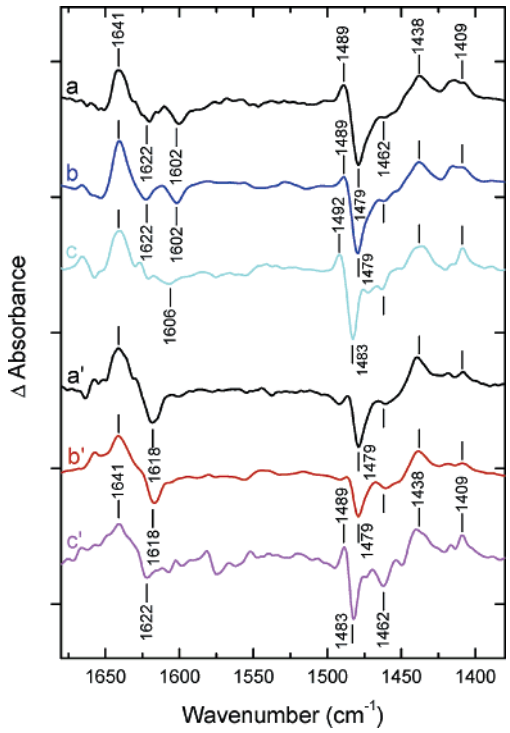

FIGURE 3: Isotope-edited IR fingerprint spectra for the interactions of Q_B and Q_B^- with the protein in *Rb. sphaeroides* RCs reconstituted with $^{13}C_1$-labeled (a−c) and $^{13}C_4$-labeled (a′−c′) UQ_3, respectively: (a and a′, black) $Q_B \rightarrow Q_B^-$ reaction at 288 K, (b, blue; b′, red) $PQ_B \rightarrow P^+Q_B^-$ reaction at 290 K, and (c, cyan; c′, magenta) $PQ_B \rightarrow P^+Q_B^-$ reaction at 85 K. The spectra have been approximately scaled. Note the same frequency of 1641 cm^{-1} for the C_1═O and C_4═O carbonyl groups of Q_B in all cases.

bonding interactions with the surrounding protein, in marked contrast to the symmetrical bonding exhibited by Q_B at room temperature.

Q_B Photoreduction at Low Temperatures. At cryogenic temperatures, charge separation to form $P^+Q_A^-$ and charge recombination to the PQ_A ground state in *Rb. sphaeroides* RCs proceed with rates and yields similar to those observed at room temperature (*14*). In contrast, the $Q_A^-Q_B \rightarrow Q_AQ_B^-$ reaction is prevented at temperatures below ∼200 K in RCs frozen in the dark, demonstrating that some activated step limits this electron transfer. The seminal work of Kleinfeld and co-workers (*14*) showed that this electron transfer step occurs at cryogenic temperatures when the RCs are cooled under illumination. In this case, the RCs become trapped in a light-adapted state in which the conformational changes that permit the $Q_A^-Q_B \rightarrow Q_AQ_B^-$ transfer are frozen-in (*14*, *39*, *40*). It follows from the data presented in Figure 2A that one way to investigate whether these conformational changes involve the distal-to-proximal movement of Q_B would be to use FTIR difference spectroscopy to examine the bonding interactions of Q_B and Q_B^- trapped at low temperatures in the light-adapted conformation, when the quinone cannot move upon photoreduction, and to compare these bonding interactions to those obtained at ambient temperature when the quinone is free to move upon photoreduction.

The same RC samples containing isotopically labeled Q_3 that were used to record the $P^+Q_B^-/PQ_B$ FTIR difference spectra at 290 K (Figure 2A) were cooled to 77 K under illumination, and were left to back-react to the PQ_B ground state in the dark at 85 K. After the sample had been allowed to equilibrate, cycles of measurements of $P^+Q_B^-/PQ_B$ FTIR difference spectra at 85 K with saturating continuous illumination were initiated. The slower rate of the back-reaction from $P^+Q_B^-$ to PQ_B observed under these conditions compared to the corresponding rate at 290 K (*14*, *39*, *40*) led to an overall reduction in the amplitude of the FTIR difference spectra under the cyclic illumination conditions. This was partially offset by increasing the delay between the individual light-minus-dark cycles of FTIR measurements.[2] The resulting FTIR difference spectra (Figure 2Ba−c) exhibit many features in common with the equivalent spectra generated at 290 K (Figure 2Aa−c), albeit with shifts of a few inverse centimeters for many of the bands. One of the largest features common to all these spectra is an increase in the amplitude of the differential signal at ∼1664(−)/1657(+) cm^{-1} in the RCs that are frozen under illumination. The same increase has been observed previously for $P^+Q_A^-/PQ_A$ spectra recorded at 100 K for *Rb. sphaeroides* RCs that were frozen under illumination (unpublished), suggesting that it represents a response of the protein in the vicinity of P.

The isotope-sensitive vibrations of Q_B and Q_B^- that involve displacement of the C_1 and C_4 atoms at 85 K are shown in the double-difference spectra for $^{13}C_1$ (Figure 2Bd) and $^{13}C_4$ (Figure 2Be) labeling. Again, all the bands that are highlighted in the double-difference spectra (Figure 2Bd,e) were observed reproducibly. In these double-difference spectra, the cancellation of some of the largest signals in the $P^+Q_B^-/PQ_B$ spectra was slightly poorer than for the equivalent sets of spectra recorded at 290 K (Figure 2Ad,e). This effect is most pronounced in the region of the 1664(−)/1656(+) cm^{-1} differential signal (Figure 2Ba,c) and is thought to represent slight variations in the response of the protein to cooling under illumination from one sample to the next or even between several cooling cycles. Small variations in the rate of cooling could explain such spurious bands.[3]

DISCUSSION

FTIR Spectroscopy Shows that both Q_B and Q_B^- Occupy the Same Position at the Proximal Site. The isotope-edited double-difference spectra for $^{13}C_1$ and $^{13}C_4$ labeling, calculated from the $P^+Q_B^-/PQ_B$ FTIR difference spectra measured at 290 and 85 K, are compiled on an expanded scale in Figure 3. Also shown in this figure are the corresponding isotope-edited double-difference spectra obtained previously (*27*) for Q_B^-/Q_B FTIR difference spectra at 288 K (Figure 3a,a′). The close agreement of the pairs of double-difference spectra measured at ambient temperature for the Q_B^-/Q_B (Figure 3a,a′) or $P^+Q_B^-/PQ_B$ (Figure 3b,b′) photoreactions is remarkable because the former spectra were measured almost 10 years ago for a different functional state of the RCs involving only Q_B and Q_B^- (*27*). Very similar spectra also have been

[2] Taking into account the amplitude of the signals in the relaxation-minus-dark $P^+Q_B^-/PQ_B$ FTIR difference spectra measured at 85 K, it is estimated that reversible charge separation occurs in 50−60% of the RCs under our experimental conditions.

[3] Confirmation of this interpretation can be obtained by calculating the variance between all the spectra measured for RCs reconstituted with a given isotopomer of UQ_3. The largest bands in the calculated variance spectra always occurred in the regions of poor cancellation observed in the double-difference spectra (Figure 2Bd, e) and were independent of the isotope label (unpublished).

observed independently for RCs that were reconstituted with $^{13}C_1$- and $^{13}C_4$-labeled UQ_{10} (*28*).

When the isotope-edited double-difference spectra for the $P^+Q_B^-/PQ_B$ reaction at 290 and 85 K for $^{13}C_1$ labeling (spectra b and c of Figure 3, respectively) or $^{13}C_4$ labeling (spectra b′ and c′ of Figure 3, respectively) are compared, the similarity of the frequencies and relative amplitudes observed for the bands assigned to Q_B and Q_B^- vibrations is striking. The most noticeable difference occurs for a negative band at 1622 cm^{-1}, which is present in the $^{13}C_1$-minus-^{12}C spectrum recorded at 290 K (Figure 3b) but is less pronounced in the spectrum measured at 85 K (Figure 3c), although this difference could be due to poor cancellation of bands in the parent $P^+Q_B^-/PQ_B$ spectra. On the other hand, most of the bands present in the spectra at 290 K have counterparts with frequencies and relative amplitudes that are closely comparable to those in the spectra obtained at 85 K, notably in the 1500−1400 cm^{-1} frequency region where the coupled C⋯O/C⋯C modes of the semiquinone absorb and where contributions from protein signals are minimal. The small variations in the frequencies and relative amplitudes of the bands are on the same order of magnitude as variations observed for many of the bands in the $P^+Q_B^-/PQ_B$ spectra recorded at the two temperatures for a given quinone isotopomer (e.g., spectra Aa and Ba of Figure 2). Although these variations could mask the presence of a limited population of Q_B (at most 15−20% considering of the noise level) in a different environment at the two temperatures, it can nevertheless be concluded that the isotope-edited IR fingerprints for the interactions of Q_B and Q_B^- with the protein binding site are closely equivalent for Q_B photoreduction at 290 and 85 K.

What is the significance of this similarity in the bonding interactions of Q_B and Q_B^- at the two temperatures? If it is assumed that the displacement of Q_B between the distal and proximal sites takes place as proposed in the conformational gating mechanism of Stowell *et al.* (*15*−*18*), then $P^+Q_B^-/PQ_B$ FTIR difference spectra measured at 290 K will probe the bonding interactions of a neutral Q_B located in the distal site (i.e., with only the C_4 carbonyl group hydrogen-bonded to the protein as depicted in Figure 1b) and of Q_B^- in the proximal site. In contrast, cooling of RCs under illumination should lead to the trapping of Q_B^- in the proximal position with a quasi-quantitative occupation of the site. Left at 85 K in the dark, this state will back-react to the PQ_B ground state without any possibility of movement of the quinone to the distal position, due to the cryogenic temperature. In this case, light-minus-dark $P^+Q_B^-/PQ_B$ FTIR difference spectra measured at 85 K probe the bonding interactions of neutral Q_B that is locked in the proximal position, in addition to a proximal Q_B^-. The frequency of the two carbonyl groups of neutral Q_B should, therefore, be noticeably different in measurements performed at the two temperatures, with notably the C_1═O carbonyl of Q_B at 290 K absorbing in the 1650−1660 cm^{-1} frequency range characteristic of a non-hydrogen-bonded group (*27*, *38*). This is inconsistent with the identical frequency of 1641 cm^{-1} found for the two carbonyl groups of Q_B at both 85 and 290 K (Figure 3). Both groups exhibit similar hydrogen bonding interactions with the protein, as originally proposed for the quinone in the proximal site of *Rp. viridis* (*27*, *29*) and as further discussed in ref *17*. The similarity of the isotope-edited IR fingerprints for the interactions of Q_B and Q_B^- with the protein measured at 85 and 290 K (Figure 3) also makes it unlikely that the quinone ring moves appreciably upon photoreduction at room temperature. It is therefore concluded that at room temperature both Q_B and Q_B^- occupy a single and unique binding site that fits well the description of the proximal site derived from X-ray crystallography (*17*, *29*, *30*). We note that the study presented here leaves open the question of the nature of the mechanism that gates the electron transfer from the primary to the secondary quinone, but a number of other possibilities have been proposed, including the dielectric response of the protein residues, internal proton shifts, and changes in the network of hydrogen bonds (*7*, *15*, *17*, *41*). In addition, the FTIR data presented here do not allow us to exclude the possibility that an energetic minimum for a quinone in the distal site exists even in functional RCs provided this quinone does not function as the genuine two-electron gate Q_B.

The conclusion that neutral Q_B in its functional state is located in the proximal site of the RC is supported by recent studies on mutant *Rb. sphaeroides* RCs that compare the location of Q_B derived from crystallographic investigations and from isotope-edited Q_B^-/Q_B FTIR spectroscopy. In several X-ray crystallographic studies at ambient temperature on dark-adapted crystals of *Rb. sphaeroides* RCs bearing mutations in the vicinity of the quinone sites, Q_B has been found to occupy the proximal position (*30*−*32*)[4] or a position intermediate between the distal and proximal sites (*31*). The isotope-edited FTIR fingerprints for the interaction of neutral Q_B with the protein have been measured for two of these mutant RCs, namely, the Pro-L209 → Tyr (*33*) and Pro-L209 → Phe (*34*) single mutants, and the bonding pattern for both the C_1═O and C_4═O carbonyls of neutral Q_B has been found to be the same as that previously measured for wild-type RCs (*27*), with two hydrogen bonds of moderate strength.[5] Note that this set of observations argues against the possibility that the C_1═O group of Q_B in wild-type RCs at ambient temperature would be shifted to 1641 cm^{-1} because of interaction with a crystallographically silent water molecule.

The evidence against a displacement of Q_B upon photoreduction that is derived here from isotope-edited FTIR difference spectroscopy parallels that previously obtained for Q_A reduction (*38*). On the basis of a comparison of crystallographic data on the location of Q_A (*3*) with EPR measurements of the distance between Q_A^- and a metal replacing the non-heme iron atom in *Rb. sphaeroides* RCs (*42*), it had been proposed that Q_A moves upon photoreduction by ∼1.5 Å toward the non-heme iron (*42*). Evidence for such a displacement was sought using Q_A-depleted *Rb. sphaeroides* RCs reconstituted with $^{13}C_1$- and $^{13}C_4$-labeled UQ_3, by comparing the isotope-edited FTIR difference spectra of $P^+Q_A^-$ formation at 100 K and of Q_A reduction

[4] The electron transfer to Q_B does not proceed when the Pro-L209 → Tyr mutant RCs with Q_B locked in the proximal position (*31*) are frozen in the dark (*41*). This supports the conclusion here that the barrier for electron transfer is a process other than quinone motion.

[5] For RCs containing the Ala-M260 → Trp mutation (*30*), the same conclusion has been reached recently Breton, J., Wakeham, W. C., Fyfe, K., Jones, M. R., and Nabedryk, E. (2004) Characterization of the bonding interactions of QB upon photoreduction via A-branch or B-branch electron transfer in mutant reaction centers from *Rhodobacter sphaeroides. Biochim. Biophys. Acta*, in press.

at 278 K. The similarity of the isotope-edited double-difference spectra for the two reactions involving Q_A and Q_A^- argued that no significant displacement of Q_A occurred upon photoreduction (*38*).

Possible Reasons for the Discrepancy with the Results from X-ray Crystallography. The location of Q_B in crystal structures of native photosynthetic bacterial RCs has long proved to be elusive. In the extensive work of Deisenhofer, Michel, and co-workers with *Rp. viridis* RCs, the Q_B site in the structural models was usually left empty (*1*, *2*, *43*). In several studies on crystals of *Rb. sphaeroides* RCs (*3*−*5*, *44*), Q_B was proposed to be located in the vicinity of what is now called the proximal site, although rather large variations were observed in the precise position of the quinone ring and the identity of its hydrogen bonding partners (*29*). Ermler *et al*. (*45*) were the first to report a quinone located in the distal site, but they presumed that it was in the ubiquinol redox state. Further improvements in the determination of the structure of *Rp. viridis* RCs with the Q_B site either depleted of quinone or reconstituted with UQ_2 led to models of Q_B in the proximal site, while refitting of earlier electron density data also favored partial occupancy of a distal site (*17*, *18*). In more recent studies, Q_B has also been proposed to bind to the distal site in a structural model of native *Rb. sphaeroides* RCs obtained at room temperature (*32*), while the most recently published model derived from the crystallographic study of *Rb. sphaeroides* RCs cryotrapped in the dark-adapted state has an approximately equal distribution of Q_B in the distal and proximal sites (*46*).

The difficulty in locating the position of Q_B precisely in structural models of RCs, while the symmetrically located and chemically identical quinone Q_A and all the other cofactors are very well defined, is likely to have more than one cause. Part of the problem is probably related to the intrinsic properties of Q_B, whose functional role as a two-electron gate and a mobile proton carrier requires a loose binding to the protein in the neutral and quinol states and a strong binding affinity in the semiquinone state[6] (*8*). Furthermore, for the neutral quinone and the ubiquinol to be able to move in and out of the Q_B binding pocket, respectively, there must be a delicate balance of hydrophobic, polar, and electrostatic interactions involving at least the polar quinone headgroup, probably the hydrophobic quinone chain, and many of the residues lining the Q_B pocket and the conduit leading to the exterior of the RC.

In the case of the RC crystals, these intrinsic difficulties linked to the functional properties of Q_B are compounded by the conditions of crystallization required for integral membrane proteins. RCs are crystallized, not only in the presence of detergent but also with high concentrations of small amphiphilic molecules (e.g., dioxane, heptanetriol) and salts (e.g., potassium phosphate, ammonium sulfate), as well as cryoprotectants for phototrapping intermediates at low temperatures. Such mixtures of chemicals could possibly interfere with the proper binding of the labile Q_B to the protein, and could explain the low occupancy of the Q_B site, or possibly even be responsible for a mispositioning of the quinone headgroup. In addition, the possibility that radiation damage by the X-ray beam could alter the redox state of the quinone, as discussed in refs *16* and *30*, has not been excluded. Another source of difficulty stems from the analysis of electron density maps with partial occupancy of the quinone site and the probable presence of water molecules in the empty site and of detergent or lipid molecules (*47*, *48*) that could be mistaken for the isoprenoid chain of Q_B.

Perhaps the most significant difference between FTIR experiments and crystallographic studies is the difficulty of ensuring that a particular redox state of Q_B is indeed being investigated under the conditions of diffraction data collection. In contrast, the conditions used here to record the $P^+Q_B^-/PQ_B$ FTIR difference spectra allow a simple control of the back-reaction kinetics of $P^+Q_B^-$ in the very same sample. When Q_B^-/Q_B FTIR difference spectra are measured with single-turnover saturating flashes in purified RCs containing a pool of added quinones, it is straightforward to use sequences of such flashes to control the period-two oscillation pattern of the semiquinone state (*36*) that is highly characteristic of Q_B functioning as a two-electron gate. Such controls are not possible with the available X-ray crystallography technology.

In conclusion, although in the past 20 years more than 40 X-ray structures of bacterial photosynthetic RCs have appeared, with a large number of these studies focusing either partially or even exclusively on the problem of the location of Q_B, no consensus about the functional relevance of the multiple quinone binding sites has been achieved. In contrast, isotope-edited FTIR difference spectroscopy shows that functional Q_B and Q_B^- occupy a single site that agrees with the description of the proximal site determined from the crystallographic studies. FTIR difference spectroscopy is exquisitely suited to the retrieval of functionally relevant local information in highly complex biological systems. However, this technique alone generally is not able to lead to a functional model without the global picture of the actual structure being derived via X-ray crystallography. This study illustrates the notable complementarity of the two approaches.

ACKNOWLEDGMENT

I am grateful to C. Boullais and C. Mioskowski for the synthesis of the labeled quinones, to P. Fyfe for preparing Figure 1, and to E. Nabedryk, M. R. Jones, and W. W. Parson for stimulating discussions.

REFERENCES

1. Deisenhofer, J., Epp, O., Miki, K., Huber, R., and Michel, H. (1984) X-ray structure analysis of a membrane protein complex. Electron density map at 3 Å resolution and a model of the chromophores of the photosynthetic reaction center from *Rhodopseudomonas viridis*, *J. Mol. Biol. 180*, 385−398.
2. Deisenhofer, J., Epp, O., Miki, K., Huber, R., and Michel, H. (1985) Structure of the protein subunits in the photosynthetic reaction centre of *Rhodopseudomonas viridis* at 3 Å resolution, *Nature 318*, 618−624.
3. Allen, J. P., Feher, G., Yeates, T. O., Komiya, H., and Rees, D. C. (1987) Structure of the reaction center from *Rhodobacter sphaeroides* R-26: The protein subunits, *Proc. Natl. Acad. Sci. U.S.A. 84*, 6162−6166.
4. El-Kabbani, O., Chang, C.-H., Tiede, D., Norris, J., and Schiffer, M. (1991) Comparison of reaction centers from *Rhodobacter sphaeroides* and *Rhodopseudomonas viridis*: Overall architecture and protein−pigment interactions, *Biochemistry 30*, 5361−5369.

[6] The tight binding of Q_B^- probably explains the well-defined position of the secondary quinone in crystals of RCs cryotrapped in the light-adapted state (*16*, *46*).

5. Feher, G., Allen, J. P., Okamura, M. Y., and Rees, D. C. (1989) Structure and function of bacterial photosynthetic reaction centres, *Nature 339*, 111−116.
6. Tiede, D. M., Vásquez, J., Córdova, J., and Marone, P. A. (1996) Time-resolved electrochromism associated with the formation of quinone anions in the *Rhodobacter sphaeroides* R26 reaction center, *Biochemistry 35*, 10763−10775.
7. Li, J., Gilroy, D., Tiede, D. M., and Gunner, M. R. (1998) Kinetic phases in the electron transfer from $P^+Q_A^-Q_B$ to $P^+Q_AQ_B^-$ and the associated processes in *Rhodobacter sphaeroides* R-26 reaction centers, *Biochemistry 37*, 2818−2829.
8. McPherson, P. H., Okamura, M. Y., and Feher, G. (1990) Electron transfer from the reaction center of *Rb. sphaeroides* to the quinone pool: Doubly reduced Q_B leaves the reaction center, *Biochim. Biophys. Acta 1016*, 289−292.
9. Okamura, M. Y., Paddock, M. L., Graige, M. S., and Feher, G. (2000) Proton and electron transfer in bacterial reaction centers, *Biochim. Biophys. Acta 1458*, 148−163.
10. Wraight, C. A. (2004) Proton and electron transfer in the acceptor quinone complex of photosynthetic reaction centers from *Rhodobacter sphaeroides*, *Front. Biosci. 9*, 309−337.
11. Arata, H., and Parson, W. W. (1981) Enthalpy and volume changes accompanying electron transfer from P-870 to quinones in *Rhodopseudomonas sphaeroides* reaction centers, *Biochim. Biophys. Acta 636*, 70−81.
12. Woodbury, N. W., and Parson, W. W. (1984) Nanosecond fluorescence from isolated photosynthetic reaction centers of *Rhodopseudomonas sphaeroides*, *Biochim. Biophys. Acta 767*, 345−361.
13. Kirmaier, C., Holten, D., and Parson, W. W. (1985) Temperature and detection-wavelength dependence of the picosecond electron-transfer kinetics measured in *Rhodopseudomonas sphaeroides* reaction centers. Resolution of new spectral and kinetic components in the primary charge-separation process, *Biochim. Biophys. Acta 810*, 33−48.
14. Kleinfeld, D., Okamura, M. Y., and Feher, G. (1984) Electron-transfer kinetics in photosynthetic reaction centers cooled to cryogenic temperatures in the charge-separated state: Evidence for light-induced structural changes, *Biochemistry 23*, 5780−5786.
15. Graige, M. S., Feher, G., and Okamura, M. Y. (1998) Conformational gating of the electron transfer reaction $Q_A^{-\bullet}Q_B \rightarrow Q_AQ_B^{-\bullet}$ in bacterial reaction centers of *Rhodobacter sphaeroides* determined by a driving force assay, *Proc. Natl. Acad. Sci. U.S.A. 95*, 11679−11684.
16. Stowell, M. H. B., McPhillips, T. M., Rees, D. C., Soltis, S. M., Abresch, E., and Feher, G. (1997) Light-induced structural changes in photosynthetic reaction center: Implications for mechanism of electron-proton transfer, *Science 276*, 812−816.
17. Lancaster, C. R. D., and Michel, H. (1997) The coupling of light-induced electron transfer and proton uptake as derived from crystal structures of reaction centres from *Rhodopseudomonas viridis* modified at the binding site of the secondary quinone, Q_B, *Structure 5*, 1339−1359.
18. Lancaster, C. R. D. (1998) Ubiquinone reduction and protonation in photosynthetic reaction centres from *Rhodopseudomonas viridis*: X-ray structures and their functional implications, *Biochim. Biophys. Acta 1365*, 143−150.
19. Alexov, E. G., and Gunner, M. R. (1999) Calculated protein and proton motions coupled to electron transfer: Electron transfer from Q_A^- to Q_B in bacterial photosynthetic reaction centers, *Biochemistry 38*, 8253−8270.
20. Grafton, A. K., and Wheeler, R. A. (1999) Amino acid protonation states determine binding sites of the secondary ubiquinone and its anion in the *Rhodobacter sphaeroides* photosynthetic reaction center, *J. Phys. Chem. B 103*, 5380−5387.
21. Rabenstein, B., Ullmann, G. M., and Knapp, E.-W. (2000) Electron transfer between the quinones in the photosynthetic reaction center and its coupling to conformational changes, *Biochemistry 39*, 10487−10496.
22. Cherepanov, D. A., Bibikov, S. I., Bibikova, M. V., Bloch, D. A., Drachev, L. A., Gopta, O. A., Oesterhelt, D., Semenov, A. Y., and Mulkidjanian, A. Y. (2000) Reduction and protonation of the secondary quinone acceptor of *Rhodobacter sphaeroides* photosynthetic reaction center: Kinetic model based on a comparison of wild-type chromatophores with mutants carrying Arg → Ile substitution at sites 207 and 217 in the L-subunit, *Biochim. Biophys. Acta 1459*, 10−34.
23. Zachariae, U., and Lancaster, C. R. D. (2001) Proton uptake associated with the reduction of the primary quinone Q_A influences the binding site of the secondary quinone Q_B in *Rhodopseudomonas viridis* photosynthetic reaction centers, *Biochim. Biophys. Acta 1505*, 280−290.
24. Walden, S. E., and Wheeler, R. A. (2002) Protein conformational gate controlling binding site preference and migration for ubiquinone-B in the photosynthetic reaction center of *Rhodobacter sphaeroides*, *J. Phys. Chem. B 106*, 3001−3006.
25. Taly, A., Sebban, P., Smith, J. C., and Ullmann, G. M. (2003) The position of Q_B in the photosynthetic reaction center depends on pH: A theoretical analysis of the proton uptake upon Q_B reduction, *Biophys. J. 84*, 2090−2098.
26. Breton, J., and Nabedryk, E. (1996) Protein-quinone interactions in the bacterial photosynthetic reaction center: Light-induced FTIR difference spectroscopy of the quinone vibrations, *Biochim. Biophys. Acta 1275*, 84−90.
27. Breton, J., Boullais, C., Berger, G., Mioskowski, C., and Nabedryk, E. (1995) Binding sites of quinones in photosynthetic bacterial reaction centers investigated by light-induced FTIR difference spectroscopy: Symmetry of the carbonyl interactions and close equivalence of the Q_B vibrations in *Rhodobacter sphaeroides* and *Rhodopseudomonas viridis* probed by isotope labeling, *Biochemistry 34*, 11606−11616.
28. Brudler, R., de Groot, H. J. M., van Liemt, W. B. S., Gast, P., Hoff, A. J., Lugtenburg, J., and Gerwert, K. (1995) FTIR spectroscopy shows weak symmetric hydrogen bonding of the Q_B carbonyl groups in *Rhodobacter sphaeroides* R26 reaction centres, *FEBS Lett. 370*, 88−92.
29. Lancaster, C. R. D., Ermler, U., and Michel, H. (1995) The structures of photosynthetic reaction centers from purple bacteria as revealed by X-ray crystallography, in *Anoxygenic Photosynthetic Bacteria* (Blankenship, R. E., Madigan, M. T., and Bauer, C. E., Eds.) pp 503−526, Kluwer Academic Publishers, Dordrecht, The Netherlands.
30. McAuley, K. E., Fyfe, P. K., Ridge, J. P., Cogdell, R. J., Isaacs, N. W., and Jones, M. R. (2000) Ubiquinone binding, ubiquinone exclusion, and detailed cofactor conformation in a mutant bacterial reaction center, *Biochemistry 39*, 15032−15043.
31. Kuglstatter, A., Ermler, U., Michel, H., Baciou, L., and Fritzsch, G. (2001) X-ray structure analyses of photosynthetic reaction center variants from *Rhodobacter sphaeroides*: Structural changes induced by point mutations at position L209 modulate electron and proton transfer, *Biochemistry 40*, 4253−4260.
32. Pokkuluri, P. R., Laible, P. D., Deng, Y.-L., Wong, T. N., Hanson, D. K., and Schiffer, M. (2002) The structure of a mutant photosynthetic reaction center shows unexpected changes in main chain orientations and quinone position, *Biochemistry 41*, 5998−6007.
33. Breton, J., Boullais, C., Mioskowski, C., Sebban, P., Baciou, L., and Nabedryk, E. (2002) Vibrational spectroscopy favors a unique Q_B binding site at the proximal position in wild-type reaction centers and in the Pro-L209 → Tyr mutant from *Rhodobacter sphaeroides*, *Biochemistry 41*, 12921−12927.
34. Nabedryk, E., Breton, J., Sebban, P., and Baciou, L. (2003) Quinone (Q_B) binding site and protein structural changes in photosynthetic reaction center mutants at Pro-L209 revealed by vibrational spectroscopy, *Biochemistry 42*, 5819−5827.
35. Okamura, M. Y., Isaacson, R. A., and Feher, G. (1975) Primary acceptor in bacterial photosynthesis: Obligatory role of ubiquinone in photoactive reaction centers from *Rhodopseudomonas sphaeroides*, *Proc. Natl. Acad. Sci. U.S.A. 72*, 3491−3495.
36. Breton, J., Berthomieu, C., Thibodeau, D. L., and Nabedryk, E. (1991) Probing the secondary quinone (Q_B) environment in photosynthetic bacterial reaction centers by light-induced FTIR difference spectroscopy, *FEBS Lett. 288*, 109−113.
37. Boullais, C., Nabedryk, E., Burie, J.-R., Nonella, M., Mioskowski, C., and Breton, J. (1998). Site-specific isotope-labeling demonstrates a large mesomeric resonance effect of the methoxy groups on the carbonyl frequencies in ubiquinones, *Photosynth. Res. 55*, 247−252.
38. Breton, J., Boullais, C., Burie, J.-R., Nabedryk, E., and Mioskowski, C. (1994) Binding sites of quinones in photosynthetic bacterial reaction centers investigated by light-induced FTIR difference spectroscopy: Assignment of the interactions of each carbonyl of Q_A in *Rhodobacter sphaeroides* using site-specific ^{13}C-labeled ubiquinone, *Biochemistry 33*, 14378−14386.
39. McMahon, B. H., Muller, J. D., Wraight, C. A., and Nienhaus, G. U. (1998) Electron transfer and protein dynamics in the photosynthetic reaction center, *Biophys. J. 74*, 2567−2587.

40. Xu, Q., and Gunner, M. R. (2001) Trapping conformational intermediate states in the reaction center protein from photosynthetic bacteria, *Biochemistry 40*, 3232−3241.
41. Xu, Q., Baciou, L., Sebban, P., and Gunner, M. R. (2002) Exploring the energy landscape for Q_A^- to Q_B electron transfer in bacterial photosynthetic reaction centers: Effect of substrate position and tail length on the conformational gating step, *Biochemistry 41*, 10021−10025.
42. Calvo, R., Passeggi, M. C. G., Isaacson, R. A., Okamura, M. Y., and Feher, G. (1990) Electron paramagnetic resonance investigation of photosynthetic reaction centers from *Rhodobacter sphaeroides* R-26 in which Fe^{2+} was replaced by Cu^{2+}. Determination of hyperfine interactions and exchange and dipole−dipole interactions between Cu^{2+} and Q_A^-, *Biophys. J. 58*, 149−165.
43. Deisenhofer, J., Epp, O., Sinning, I., and Michel, H. (1995) Crystallographic refinement at 2.3 Å resolution and refined model of the photosynthetic reaction centre from *Rhodopseudomonas viridis*, *J. Mol. Biol. 246*, 429−457.
44. Arnoux, B., and Reiss-Husson, F. (1996) Pigment−protein interactions in *Rhodobacter sphaeroides* Y photochemical reaction center; comparison with other reaction center structures, *Eur. Biophys. J. 24*, 233−242.
45. Ermler, U., Fritzsch, G., Buchanan, S. K., and Michel, H. (1994) Structure of the photosynthetic reaction centre from *Rhodobacter sphaeroides* at 2.65 Å resolution: Cofactors and protein−cofactor interactions, *Structure 2*, 925−936.
46. Fritzsch, G., Koepke, J., Diem, R., Kuglstatter, A., and Baciou, L. (2002) Charge separation induces conformational changes in the photosynthetic reaction centre of purple bacteria, *Acta Crystallogr. D58*, 1660−1663.
47. McAuley, K. E., Fyfe, P. K., Ridge, J. P., Isaacs, N. W., Cogdell, R. J., and Jones, M. R. (1999) Structural details of an interaction between cardiolipin and an integral membrane protein, *Proc. Natl. Acad. Sci. U.S.A. 96*, 14706−14711.
48. Camara-Artigas, A., Brune, D., and Allen, J. P. (2002) Interactions between lipids and bacterial reaction centers determined by protein crystallography, *Proc. Natl. Acad. Sci. U.S.A. 99*, 11055−11060.

BI049811W